JACS
JOURNAL OF THE AMERICAN CHEMICAL SOCIETY
Article
pubs.acs.org/JACS

Three Distinct Equilibrium States via Self-Assembly: Simple Access to a Supramolecular Ion-Controlled NAND Logic Gate

Dong Sub Kim,[†] Vincent M. Lynch,[†] Jung Su Park,*[,§] and Jonathan L. Sessler*[,†,‡]

[†]Department of Chemistry and Biochemistry, The University of Texas at Austin, Austin, Texas 78712-1224, United States
[§]Department of Chemistry, Sookmyung Woman's University, Seoul 140-742, Korea
[‡]Department of Chemistry, Yonsei University, Seoul 120-749, Korea

Supporting Information

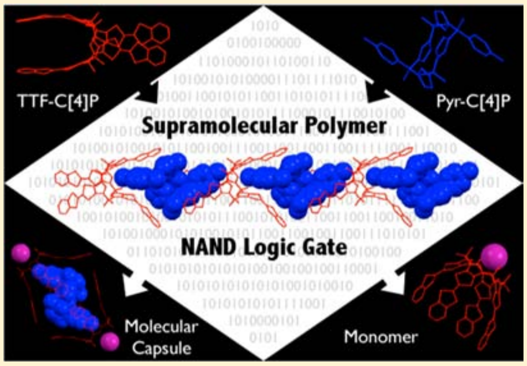

ABSTRACT: During the past several decades, considerable effort has focused on self-assembled systems. However, most work has been directed toward understanding the equilibrium between two major chemical entities, namely the dissociated components and the corresponding associated complex. While there are quite a few examples of 'multi-responsive' materials, control over 'multistate' materials has proved difficult to achieve. Here, we report the formation and the interplay of a self-assembled calix[4]pyrrole array that exhibits three limiting forms, namely a 1:1 self-assembled oligomer, a 2:1 capsule, and the corresponding monomers. Interconversion between these states may be controlled by using the tetraethylammonium cation (TEA$^+$) and/or iodide anion (I$^-$) as chemical inputs. The combination of self-assembly and ion-based control may be used to create systems that display NAND logic behavior. The system outputs have been confirmed by a variety of analytic methods, including UV–vis and 2D ^{1}H DOSY, NOESY NMR spectroscopy, scanning electron microscopy, and single crystal X-ray diffraction analyses.

INTRODUCTION

The appeal of nanoscale computing and molecular informatics is driving efforts to store and read out information at the molecular level. Inspired by this challenge, considerable effort has been invested in developing molecular systems that allow access to more than two equilibrium states. This has led to such elegant systems as multistation mechanically linked rotaxanes,[1] coordination arrays,[2] and photochromic molecules.[3] An appealing and labor saving alternative would be multimode systems generated via self-assembly. Such systems could consist of supramolecular ensembles that permit reversible and controllable access to multiple molecular states via an appropriate choice of external inputs. To date, self-assembly has been effectively used to create nanostructured materials,[4,5] support dynamic combinatorial chemistry,[6] and produce supramolecular polymers.[7,8] For instance, synthetic supramolecular polymeric systems have been exploited to create a variety of functional materials including, but not limited to, self-healing,[9] stimuli-responsive,[10] and sensory materials.[11] However, this approach has yet to be used to produce self-assembled supramolecular polymers that display NAND-logic gate behavior. We believe that such systems may be obtained by creating self-assembled ensembles that allow access to three discrete states that may be interconverted via application of appropriate chemical inputs. Herein, we report a three-state system that can be prepared by simple mixing. Specifically, we detail the preparation of a self-assembled system based on two different calix[4]pyrrole (C[4]P) subunits that exists in three limiting equilibrium states (monomer, capsule, and oligomer). This system undergoes ion-dependent conversion to three different molecular states as the result of controlled changes in the conformations of the constituent C[4]Ps. This gives rise to various spectroscopically distinct chemical products (output) based on the choice of the ion (input) and does so in accord with the terms of a NAND logic operation. (Note: A NAND gate is defined as a logic gate that produces a "false" response only if all inputs are true.)[12,13] The present system differs from other NAND logic devices, both in terms of its ease of preparation and by virtue of the fact that the same output is produced from two of three underlying states, namely a supramolecular oligomeric structure and a molecular capsule. It also differs from other well-characterized multistate systems in that it does not rely on the use of either covalent or mechanical bonds.

Calix[4]pyrroles are attractive receptors for the generation of stimulus-controlled self-assembled structures, including as detailed below NAND logic devices. Calix[4]pyrroles are nonaromatic tetrapyrrolic macrocycles that typically undergo a dramatic conformational change from the more thermodynamically stable 1,3-alternate conformation to a bowl-like cone conformation upon the addition of coordinating anions, such as carboxylate, sulfate, phosphate, and halides.[14−16] The C[4]Ps are also of interest because in their respective cone

Received: August 2, 2013
Published: September 5, 2013

dx.doi.org/10.1021/ja4080198 | *J. Am. Chem. Soc.* 2013, 135, 14889−14894

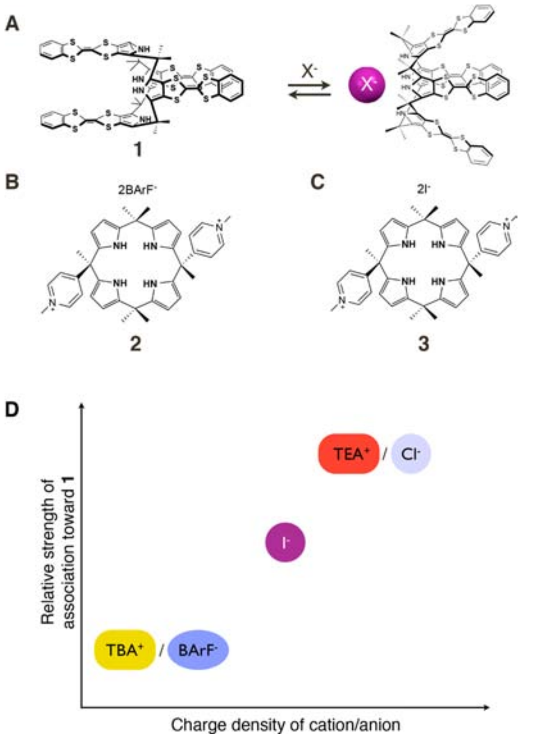

Figure 1. Chemical structures of three C[4]P species used in the present study. (A) The TTF-functionalized C[4]P (TTF-C[4]P, **1**) acts as a switching unit through anion and/or cation recognition. (B) and (C) The two building blocks with which **1** is allowed to interact in a noncovalent fashion, namely, a bismethylpyridinium-functionalized C[4]P as the bis-BArF (anions omitted for clarity) and the bis-iodide salts (species **2** and **3**, respectively). (D) Schematic illustration of the relative binding affinity of relevant anions and cations for **1** plotted vs the charge density of the ion in question.

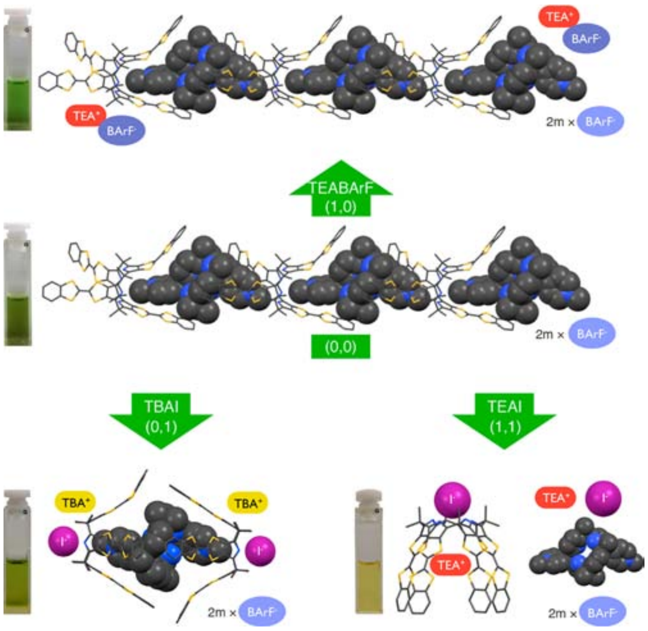

Figure 2. Schematic representation of the three limiting equilibrium states produced from **1** and **2** via treatment with appropriate ions. These states are illustrated starting from the self-assembled NAND logic gate $(\mathbf{1}\cdot\mathbf{2})_n$. The logic operations are triggered via the addition of various tetraalkylammonium salts (2 equiv each) as inputs. Also shown are the structures corresponding to the resulting outputs as observed in chloroform solution (where *m* is the number of equivalents of **2** present in solution).

conformations (as produced in the presence of a strongly coordinating anion) they will bind moderately sized cations, such as Cs^+ and tetraethylammonium cation (TEA^+), but not larger species, such as the tetrabutylammonium cation (TBA^+).[17,18] These features make the C[4]Ps attractive as building blocks for the creation of self-assembled materials. In particular, disparities in binding affinities, arising from differences in size and charge density, could be exploited to control the nature of C[4]P-derived self-assembled materials.

In a recent study, we showed the formation of supramolecular polymers from two different C[4]Ps, wherein the main attractive forces were hydrogen-bonding and charge-transfer interactions.[11] These self-assembled polymeric arrays were found to exhibit an environmental response, undergoing deaggregation when exposed to analytes such as trinitrobenzene (TNB) and chloride anion. In separate work, we demonstrated that electron transfer between an electron-rich TTF-annulated C[4]P and an electron-poor acceptor, such as bisimidazolium quinone (BIQ^{2+})[19] or Li@C_{60},[20] could be regulated via the addition of anions or cations. As a general rule, conformation change-driven switching is induced by the formation of pyrrole NH-anion hydrogen bonds, with smaller and more highly charge dense anions binding more tightly.[14]

Based on the above precedent, we considered it likely that a new supramolecular NAND logic device could be constructed via the use of two different C[4]Ps whose response to added anions and cations is slightly different. As detailed below, this objective was achieved by using a tetrathiafulvalene (TTF)-functionalized C[4]P (TTF-C[4]P, **1**) in conjunction with two appropriately chosen *trans*-bis(methylpyridinium)-*meso*-substituted C[4]P salts, namely Pyr-C[4]P **2** and Pyr-C[4]P **3**. These two salts are comprised of the same C[4]P dication but differ in the nature of counteranions. Whereas **2** contains two noncoordinating tetrakis[bis(3,5-trifluoromethyl)phenyl]borate ($BArF^-$) anions,[21−23] **3** bears two more strongly bound iodide counteranions. The structural changes induced by varying these anions and their salt forms give rise, in turn, to different colors in $CDCl_3$ solution, thus producing "readouts" that conform to NAND logic behavior. The various components of the present NAND system are shown in Figure 1. The underlying chemistry is summarized in Figure 2.

■ FORMING A SUPRAMOLECULAR OLIGOMER AND CREATING A FIRST EQUILIBRIUM STATE

When mixed in chloroform, **1** and **2** self-assemble to form a supramolecular oligomeric material, $(\mathbf{1}\cdot\mathbf{2})_n$, that is stabilized by donor−acceptor interactions between the electron-rich TTF moieties present in compound **1** and the electron-poor methylpyridinium units of compound **2**. In the absence of a coordinating anion (i.e., using the BArF salt **2**), each C[4]P exists in the 1,3-alterante conformation such that the electron-deficient pyridinium units are intercalated within the cavity generated by two electron-rich TTF moieties. Such behavior is consistent with what is normally observed for C[4]Ps and matches what was seen in a previous study wherein a bis-dinitrophenyl-functionalized C[4]P was found to be stabilized in the form of a sandwich-like complex in the presence of a second C[4]P that contains TTF subunits.[11]

An immediate change in color accompanies the mixing of **1** and **2** (yellow to green) with corresponding differences in the

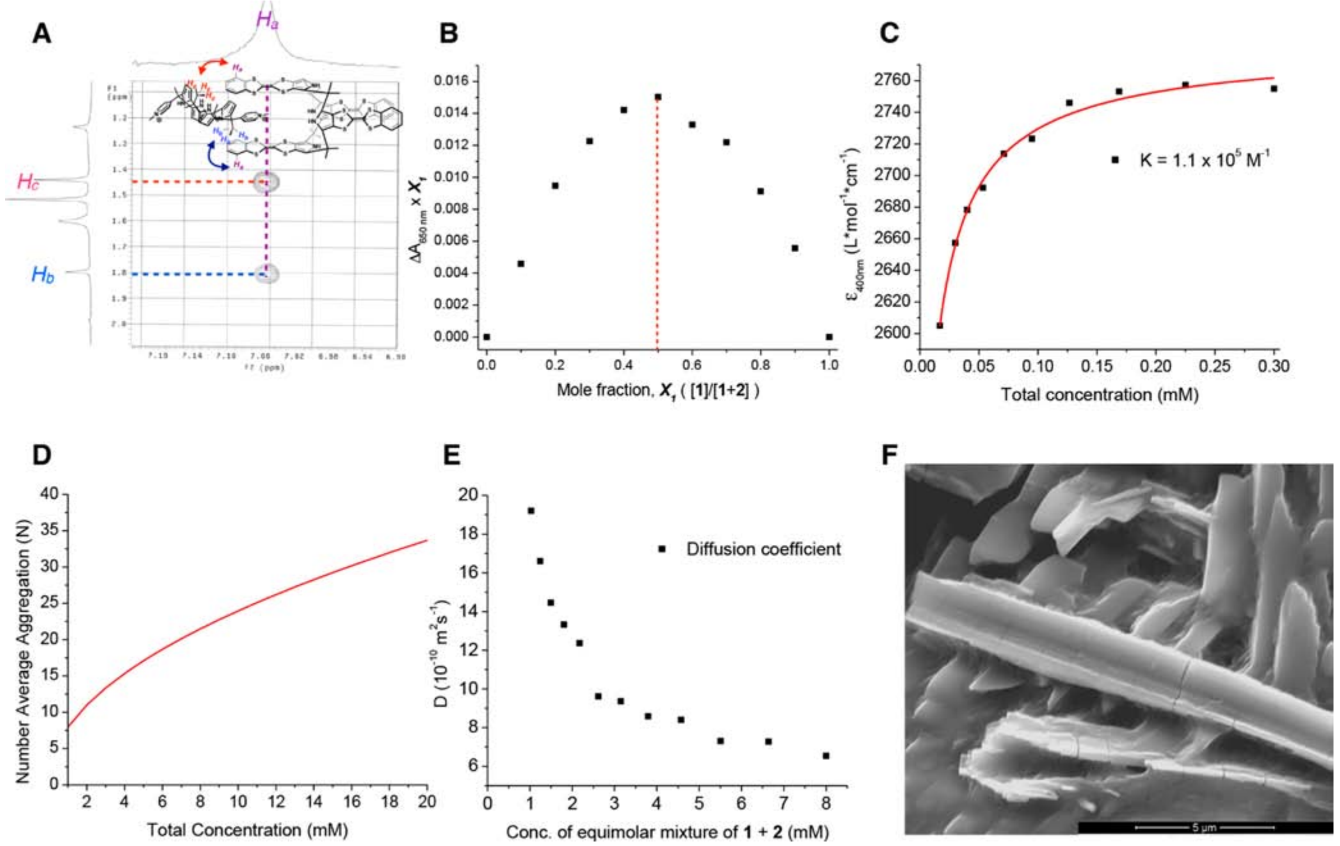

Figure 3. Results of studies that provide support for the formation of a self-assembled ensemble $(\mathbf{1}\cdot\mathbf{2})_n$. (A) Partial ^{1}H NOESY NMR spectra of $(\mathbf{1}\cdot\mathbf{2})_n$, highlighting the intermolecular coupling patterns between **1** and **2**. (B) Continuous variation plot for a 1:1 mixture of **1** and **2**. These plots were constructed by plotting the product of the change in the absorption at 650 nm and the mole fraction of **1** vs the mole fraction of **1**. (C) Plot of molar extinction coefficient as a function of the total concentration of an equimolar mixture of **1** and **2**. (D) Simulation of the number average aggregate size based on the calculated binding constant, $K_a = 1.1 \times 10^5$ M^{-1}. (E) Change in diffusion coefficient seen upon dilution of a chloroform mixture of $(\mathbf{1}\cdot\mathbf{2})_n$. (F) SEM images of $(\mathbf{1}\cdot\mathbf{2})_n$. This form corresponds to the self-assembled NAND gate (first equilibrium state) noted in the text.

UV–vis spectrum being seen (e.g., appearance of a CT band at 650 nm). Such noticeable color changes are not seen when simple solutions of TTF and the pyridinium salt **2** are mixed at the same concentration as used in the case of **1** and **2** (cf. Figure S10). On this basis, we propose that formation of the putative self-assembled material involves interactions between the two macrocyclic components.

To characterize further the putative oligomer $(\mathbf{1}\cdot\mathbf{2})_n$, an ^{1}H-NOESY NMR analysis was carried out in CDCl$_3$ solution (Figure 3A). The occurrence of cross-peaks corresponding to through-space interactions of protons from **1** and **2** was seen. A continuous variation study (so-called Job plot analysis), performed by plotting the product of the change in absorption at 650 nm (ΔA) and the mole fraction of **1** (X_1) (Y-axis) as a function of mole fraction of **1** (X_1) (X-axis) gave a symmetric curve, that displayed a maximum value at $X_1 = 0.5$ (Figure 3B). Taken together, these findings are consistent with a self-assembled system with an effective 1:1 stoichiometry for the “monomers” **1** and **2**. However, these analyses provide no insight into the average size of the presumed oligomer (i.e., the effective value of n in $(\mathbf{1}\cdot\mathbf{2})_n$).

To obtain insights into the average length of the proposed linear ensemble formed from **1** and **2**, a plot of the extinction coefficients as a function of total concentration of $(\mathbf{1}\cdot\mathbf{2})_n$ was constructed; this yielded a smooth hyperbolic curve. The effective binding affinity was then calculated based on a modified equal K model.[11] Specifically, a nonlinear curve fitting analysis using an isodesmic model provided an affinity constant of 1.1×10^5 M^{-1} in chloroform solution for the interaction between **1** and **2** (Figure 3C). On this basis, the average value of n was determined to be ~23 at a 10 mM total concentration (i.e., [**1**] and [**2**] = 5 mM, respectively; Figure 3D).[11,24]

Further evidence for the formation of a linear oligomer came from concentration-dependent diffusion ordered (DOSY) NMR spectroscopic studies carried out in CDCl$_3$ (Figure 3E). For a two-component system undergoing self-assembly to provide a larger aggregate, the value of the diffusion coefficient is expected to vary inversely in proportion to the net concentration of the monomeric constituents. In accord with this expectation, reduced diffusion coefficients were observed as the total concentration of an equimolar solution of **1** and **2** was increased. On the basis of these solution-state data, it is concluded that the self-assembled ensemble produced by mixing **1** and **2** in a 1:1 molar ratio exists in the form of a 1D oligomer of generalized structure $(\mathbf{1}\cdot\mathbf{2})_n$ in CDCl$_3$, even at relatively low concentrations.

In order to investigate the morphology of this system in the solid state, scanning electron microscope (SEM) studies were carried out. Microcrystalline material, obtained via the slow evaporation of what was originally a solution of $(\mathbf{1}\cdot\mathbf{2})_n$ in chloroform, was examined. SEM images revealed long, needle-shaped microstructures as would be expected for a material comprised of a 1D assembly (Figure 3F).

A

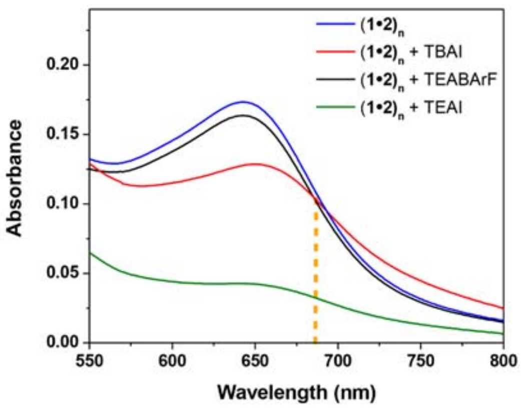

B

Condition	In_1 TEA^+	In_2 I^-	Out (Norm. value at 690 nm)
$(1\cdot2)_n$	0	0	1 (1.00)
$(1\cdot2)_n$ + TEA^+ + $BArF^-$	1	0	1 (0.97)
$(1\cdot2)_n$ + TBA^+ + I^-	0	1	1 (0.92)
$(1\cdot2)_n$ + TEA^+ + I^-	1	1	0 (0.00)

Figure 4. Logic Operations. (A) CT response of the self-assembled NAND gate $(\mathbf{1}\cdot\mathbf{2})_n$ seen when the iodide anion (I^-) and the tetraethylammonium (TEA^+) cation are added as inputs. (B) Truth table. Note that both I^- and TEA^+ are required to produce a "0" output.

■ ACCESSING TWO OTHER EQUILIBRIUM STATES AND PERFORMING NAND LOGIC OPERATIONS

Having this self-assembled species $(\mathbf{1}\cdot\mathbf{2})_n$ in hand, various alkylammonium salts were added. These disparate salts were expected perturb the system in accord with a NAND logic operation. This expectation was realized when the binary chemical inputs are the iodide anion (I^-) and the tetraethylammonium cation (TEA^+). The iodide anion could be introduced to $(\mathbf{1}\cdot\mathbf{2})_n$ in $CDCl_3$ in the form of its tetrabutylammonium or tetraethylammonium salt (TBAI and TEAI, respectively). The second input, TEA^+ could be added as its $BArF^-$ or iodide anion salt (TEABArF and TEAI, respectively). Since neither the $BArF^-$ anion nor the TBA^+ cation interacts with C[4]Ps appreciably, they were expected to be inactive components in terms of inducing logic operation changes in the case of the proposed NAND gate consisting of $(\mathbf{1}\cdot\mathbf{2})_n$.

Without any input—the (0,0) case—the NAND gate $(\mathbf{1}\cdot\mathbf{2})_n$ (i.e., first equilibrium state described above) displays a maximal intensity for the charge-transfer (CT) band at 690 nm in the presence of the noncoordinating $BArF^-$ anions. This intensity was normalized to 1 and corresponds to a logic operation output of 1. Upon the addition of TEABArF (the (1,0) situation), the intensity of the 690 nm CT band is not significantly perturbed (normalized value: 0.97). Since $BArF^-$ does not induce the conformational change needed to convert **1** from its 1,3-alternate conformation to the corresponding cone form, there is no bowl-like cavity into which the TEA^+ cation may bind. Therefore, the addition of TEABArF to the NAND gate $(\mathbf{1}\cdot\mathbf{2})_n$ also produces an output of 1.

In the case of TBAI, corresponding to a (0,1) situation, the addition of I^- brings a conformational change and leads to binding of the anion via hydrogen-bonding interactions with the pyrrolic NH protons of **1**. This produces a bowl-like cavity into which the bismethylpyridnium-functionalized C[4]P **2** associates with two equivalents of $[\mathbf{1}\cdot I]^-$ to give a strongly associated molecular capsule (Figure 2). This newly self-assembled molecular capsule, corresponding to a second equilibrium state, also shows a charge transfer interaction (normalized value: 0.92).

Support for the proposed molecular capsule, $\mathbf{1}_2\cdot\mathbf{3}$, came via a single crystal X-ray diffraction analysis using crystals grown via the slow evaporation of a chloroform/ethanol mixture containing **1** and **3** (Figure 5A). The two subunits of **1** seen in the solid state face each other and create a capsule-like arrangement into which one equivalent of **3** is bound. The methylpyridinium groups of **3** are oriented inside the cone of **1** to form what can be viewed as being receptor-separated ion-pair complexes involving iodide anions that are hydrogen-bonded to the C[4]P NH protons of **1**. In the solid state, the molecular capsule appears to be stabilized by several types of noncovalent interactions. These include: (i) CT interactions between the electron-rich TTF moieties in **1** and the electron-deficient methylpyridinium subunits in **3**; (ii) CH$\cdots\pi$ interactions between the aromatic pyridinium C−H protons and the π surfaces of the TTF subunits (average distance: 2.54 Å) as well as the sp^3 pyridinium-CH_3 and pyrrolic π surface of **1** (average distance: 2.66 Å); and (iii) ion-pairing interactions between cationic pyridinium and anionic I^- (average distance: 6.75 Å).

The molecular capsule $\mathbf{1}_2\cdot\mathbf{3}$ was further analyzed in chloroform solution. In this solvent, a Job's plot revealed a 2:1 stoichiometry between **1** and **3** in solution as seen in the crystal structure (Figure S11a). A UV−vis spectroscopic-based Job plot involving monitoring the change in absorbance at 470 nm revealed a maximum value at a mole fraction X_1 of 0.7. A separate plot of the change in absorbance at 470 nm vs concentration yielded a binding isotherm that could be fit well to a 2:1 binding model; this yielded values for $K_1 = 8.1 \times 10^3$ M^{-1} and $K_2 = 1.1 \times 10^3$ M^{-1} (Figure S11b). These association constants proved larger than those corresponding to the formation of [**1**·TBAI] alone (4.8×10^2 M^{-1}), as calculated in a separate experiment (Figure S12b). This latter finding provides a rationale for why the addition of TBAI to a mixture of **1** and **2** leads to formation of a molecular capsule; the alternative, where the TBA^+ cation, rather than the methylpyridinium-functionalized C[4]P, binds preferentially to the iodide anion stabilized cone conformer of **1** is ruled out on thermodynamic grounds.

The final input, namely TEAI, serves to dismantle the oligomer $(\mathbf{1}\cdot\mathbf{2})_n$ and break it up into its "monomers". Typically, the iodide anion does not coordinate strongly to C[4]Ps because it has a relatively large ionic radius and a charge density that is correspondingly lower than, e.g., the chloride anion. However, the absolute K_a value corresponding to the association depends on many factors, including the choice of countercation. Specifically, when TEA^+ is used, the association between **1** and TEAI is strong ($K_a = 1.5 \times 10^5$ M^{-1} in chloroform solution). This relatively high K_a value reflects the fact that, in contrast to the TBA^+ cation, the TEA^+ cation can fit within the cone of C[4]Ps.[18,25] The addition of TEAI to the NAND gate $(\mathbf{1}\cdot\mathbf{2})_n$ thus causes near-complete dissociation of

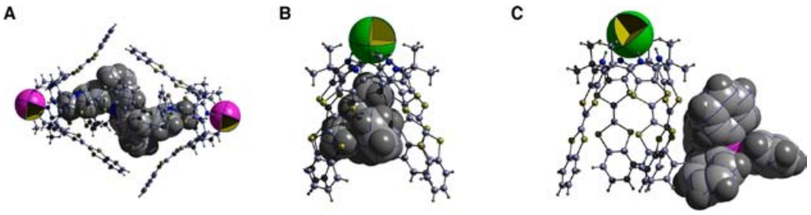

Figure 5. X-ray single crystal structures of (A) molecular capsule, $\mathbf{1}_2\cdot\mathbf{3}$, (B) cation-included complex **1**·TEACl, and (C) the cation-excluded congener, **1**·TPPCl.

the system and produces a third equilibrium state consisting of the isolated "monomers". This disassembly leads to a significant loss of intensity in the case of the CT band at 690 nm (normalized intensity: 0) as well as an easy-to-see change in the color of the solution. As a consequence, adding TEAI produces a 0 or "false" as an output; this corresponds to a (1,1) logic situation. All logic operations, the sum total of which correspond to a NAND gate, are summarized in Figure 4.[26]

Additional support for the proposed ion pair monomeric complexes (i.e., third equilibrium state) produced as the result of the TEAI-induced deaggregation of $(\mathbf{1}\cdot\mathbf{2})_n$ came from an X-ray diffraction analysis of crystals **1**·TEACl (Figure 5B). In accord with what had been observed in the case of other, simpler C[4]Ps, macrocycle **1** was found to adopt the cone conformation within the complex with the chloride anion being bound to the pyrrole NH protons through hydrogen bonds. This structure also revealed that the relatively small tetraalkylammonium cation, TEA^+, is cocomplexed within the concave, bowl-like cavity, presumably being stabilized in its binding by cation−π interactions. In contrast, a corresponding structure, obtained from crystals of the corresponding tetraphenylphosphonium chloride (TPPCl) salt of **1**, revealed that the tetraphenylphosphonium (TPP^+) cation is not bound within the C[4]P cavity (cf. Figure 5C). Rather, the TPP^+ cation is only loosely associated with the chloride anion complex. These structural findings are thus fully consistent with the suggestion that the size of the countercation plays a critical role in regulating the equilibrium states obtained in mixtures consisting of **1** and **2** and thus the NAND response seen with the starting oligomeric logic gate $(\mathbf{1}\cdot\mathbf{2})_n$.

CONCLUSION

In summary, we have shown that the appropriate use of two disparate ion-responsive C[4]Ps allows controlled access to three different equilibrium states in chloroform solution. Simple mixing of **1** and **2** leads to formation of a self-assembled supramolecular array $(\mathbf{1}\cdot\mathbf{2})_n$ that is stabilized via CT interactions between the TTF subunits and methylpyridinium groups on the constituent C[4]Ps. This ensemble functions as a NAND molecular logic device, whose operation is made possible by the unique ion binding features displayed by functionalized C[4]Ps. Each output operation, as well as the null set, was analyzed using various spectroscopic and structural methods, including UV−vis and 2D ^1H DOSY, NOESY NMR spectroscopy, SEM, and X-ray single crystal analyses. This has allowed three limiting forms, namely a 1:1 self-assembled oligomer, a 2:1 capsule, and the monomers to be fully defined. Their interplay, which is carefully controlled through ion-based inputs, serves to create a NAND logic gate without resorting to the use of either mechanical or covalent bonds to modulate the underlying multistate switching process. The simplicity of the present system provides a potentially attractive approach to the creation of molecular logic devices accessible by supramolecular assembly.

ASSOCIATED CONTENT

Supporting Information

Experimental procedures, UV−vis spectroscopic data, 2D ^1H DOSY, NOESY NMR spectra, scanning electron microscopic data, X-ray single crystallographic data. This material is available free of charge via the Internet at http://pubs.acs.org.

AUTHOR INFORMATION

Corresponding Authors

jspark@sookmyung.ac.kr
sessler@cm.utexas.edu

Notes

The authors declare no competing financial interest.

ACKNOWLEDGMENTS

This research was supported by the U.S. National Science Foundation (CHE-1057904), the Robert A. Welch Foundation (F-1018), the World Class University (WCU) (R32-2012-000-10217-0) and Basic Science Research Programs through the National Research Foundation of Korea (NRF) funded by the Ministry of Science, ICT and Future Planning (2013R1A1A1011508).

REFERENCES

(1) Qu, D. -H.; Wang, Q.-C.; Ma, X.; Tian, H. *Angew. Chem., Int. Ed.* **2005**, *44*, 5296−5299.

(2) Semenov, A.; Spatz, J. P.; Möller, M.; Lehn, J. −M.; Sell, B.; Schubert, D.; Weidl, C. H.; Schubert, U. S. *Angew. Chem., Int. Ed.* **1999**, *38*, 2547−2550.

(3) Pina, F.; Roque, A.; Melo, M. J.; Maestri, M.; Belladelli, L.; Balzani, V. *Chem.−Eur. J.* **1998**, *4*, 1184−1191.

(4) Boal, A. K.; Ilhan, F.; DeRouchey, J. E.; Thurn-Albrecht, T.; Russell, T. P.; Rotello, V. M. *Nature* **2000**, *404*, 746−748.

(5) Black, C. T.; Murray, C. B.; Sandstrom, R. L.; Sun, S. *Science* **2000**, *290*, 1131−1134.

(6) Corbett, P. T.; Leclaire, J.; Vial, L.; West, K. R.; Wietor, J. −L.; Sanders, J. K. M.; Otto, S. *Chem. Rev.* **2006**, *106*, 3652−3711.

(7) De Greef, T. F. A.; Smulders, M. M. J.; Wolffs, M.; Schenning, A. P. H. J.; Sijbesma, R. P.; Meijer, E. W. *Chem. Rev.* **2009**, *109*, 5687−5754.

(8) De Greef, T. F. A.; Meijer, E. W. *Nature* **2008**, *453*, 171−173.

(9) Cordier, P.; François Tournilhac, F.; Soulié-Ziakovic, C.; Leibler, L. *Nature* **2008**, *451*, 977−980.

(10) Wojtecki, R. J.; Meador, M. A.; Rowan, S. J. *Nat. Mater.* **2011**, *10*, 14−27.

(11) Park, J. S.; Yoon, K. Y.; Kim, D. S.; Lynch, V. M.; Bielawski, C. W.; Johnston, K. P.; Sessler, J. L. *Proc. Natl. Acad. Sci. U.S.A.* **2011**, *108*, 20913−20917.

(12) For seminal studies of molecular logic devices, please see: (a) Aviram, A. *J. Am. Chem. Soc.* **1998**, *110*, 5687−5692. (b) de Silva, P. A.; Gunaratne, N. H. Q.; McCoy, C. P. *Nature* **1993**, *364*, 42−44.

(13) For examples of NAND logic gates, please see: (a) Saghatelian, A.; Völcker, N. H.; Guckian, K. M.; Lin, V. S. −Y.; Ghadiri, M. R. *J. Am. Chem. Soc.* **2003**, *125*, 346−347. (b) Baytekin, H. T.; Akkaya, E. U. *Org. Lett.* **2000**, *2*, 1725−1727.

(14) Gale, P. A.; Sessler, J. L.; Král, V.; Lynch, V. M. *J. Am. Chem. Soc.* **1996**, *118*, 5140−5141.

(15) Allen, W. E.; Gale, P. A.; Brown, C. T.; Lynch, V. M.; Sessler, J. L. *J. Am. Chem. Soc.* **1996**, *118*, 12471−12472.

(16) Gale, P. A.; Sessler, J. L.; Král, V. *Chem. Commun.* **1998**, 1−8.

(17) Custelcean, R.; Delmau, L. H.; Moyer, B. A.; Sessler, J. L.; Cho, W. −S.; Gross, D.; Bates, G. W.; Brooks, S. J.; Light, M. E.; Gale, P. A. *Angew. Chem., Int. Ed.* **2005**, *44*, 2537−2542.

(18) Sessler, J. L.; Gross, D. E.; Cho, W. −S.; Lynch, V. M.; Schmidtchen, F. P.; Bates, G. W.; Light, M. E.; Gale, P. A. *J. Am. Chem. Soc.* **2006**, *128*, 12281−12288.

(19) Park, J. S.; Karnas, E.; Ohkubo, K.; Chen, P.; Kadish, K. M.; Fukuzumi, S.; Bielawski, C. W.; Hudnall, T. W.; Lynch, V. M.; Sessler, J. L. *Science* **2010**, *329*, 1324−1327.

(20) Fukuzumi, S.; Ohkubo, K.; Kawashima, Y.; Kim, D. S.; Park, J. S.; Jana, A.; Lynch, V. M.; Kim, D.; Sessler, J. L. *J. Am. Chem. Soc.* **2011**, *133*, 15938−15941.

(21) The BArF$^-$ anion has a far lower coordinating ability than PF_6^-, BF_4^-, or ClO_4^-.

(22) For more information on weakly coordinating anions, please see: Korssing, I.; Raabe, I. *Angew. Chem., Int. Ed.* **2004**, *43*, 2066−2090.

(23) Nishida, H.; Takada, N.; Yoshimura, M.; Sonoda, T.; Kobayashi, H. *Bull. Chem. Soc. Jpn.* **1984**, *57*, 2600−2604.

(24) Brunsveld, L.; Folmer, B. J. B.; Meijer, E. W.; Sijbesma, R. P. *Chem. Rev.* **2001**, *101*, 4071−4097.

(25) Gross, D. E.; Schmidtchen, F. P.; Antonius, W.; Gale, P. A.; Lynch, V. M.; Sessler, J. L. *Chem.−Eur. J.* **2008**, *14*, 7822−7827.

(26) Effort to produce the same logic operations using TEA$^+$ and Cl$^-$ as binary inputs failed. This failure is ascribed to the fact that the Cl$^-$ anion binds too strongly not only to **1** but also to **2** such that no switching is possible upon changing the countercation. In fact, the K_a for the binding of Cl$^-$ (as its TBACl salt) to **1** (and **2** as well) is similar in magnitude to, or even greater than, the affinity between **1** and **2** (cf. Figures S12−13).